

Dual Polarization Radar Signal Processing

Second Semester Report
2006-2007

by
Joe Hoatam
Josh Merritt
Aaron Nielsen

Prepared to partially fulfill the requirements for
EE401/EE402

Department of Electrical and Computer Engineering
Colorado State University
Fort Collins, Colorado 80523

Report Approved: _____

Project Advisor

Senior Design Coordinator

ABSTRACT

Dual polarization radar signal processing is the processing of data with a horizontal and a vertical component obtained from received radar signals. Several issues such as clutter, range ambiguity, and velocity ambiguity need to be addressed when processing data from radars. Joe Hoatam is studying clutter, Aaron Nielsen is studying range ambiguity, and Josh Merritt is studying velocity ambiguity. Radar signal processing is important and utilized in military, weather, and civilian applications.

In the first semester, we studied the basics of dual polarization radar signal processing in depth and then began to research techniques to solve the issues involved in the area. Ground clutter can be tackled by using notch FIR or IIR filters. A technique called GMAP can also be utilized in the removal of clutter. Range ambiguity can be addressed using phase coding. Phase codes such as systematic codes and random phase codes were used in the past and today, SZ codes are being implemented for better results. For the problem of velocity ambiguity, multiple pulse repetition frequencies (prf) can be used in conjunction with clustering algorithms and the maximum likelihood algorithm.

In the second semester, we proceeded by analyzing the techniques first hand, whether by simulation or actual data analysis. Using data collected from the CASA radar, clutter suppression was studied using the GMAP algorithm. As for lowering the effects of range ambiguity, data collected by the CHILL radar was phase coded and conclusions were drawn from the results. Finally, velocity ambiguity mitigations were researched and simulated via clustering and maximum likelihood algorithms.

TABLE OF CONTENTS

Title	1
Abstract	2
Table of Contents	3
List of Figures and Tables	4
1 Introduction	5
2 Simulation Results	9
3 Clutter	15
3.1 Overview	15
3.2 Solution Researched	17
3.3 Conclusion	22
4 Range Ambiguity	24
4.1 Overview	24
4.2 Solution Researched	27
4.3 Conclusion	37
5 Velocity Ambiguity	39
5.1 Overview	39
5.2 Solution Researched	40
5.3 Conclusion	44
6 Conclusions and Future Work	45
7 References	47
8 Bibliography	48
A1 Appendix – Relevant Matlab Codes	49
A2 Additional considerations	54
A3 Acknowledgements	55

LIST OF FIGURES

Figure 1	Radar Illustration	5
Figure 2	Mean Power vs. Velocity (Rectangular Window)	9
Figure 3	Mean Power vs. Velocity (Hamming Window)	10
Figure 4	Mean Power vs. Velocity (Blackman Window)	10
Figure 5	Mean Power vs. Sample Size	11
Figure 6	Mean Velocity vs. Sample Size	12
Figure 7	Standard Deviation of Power vs. Sample Size	12
Figure 8	Standard Deviation of Velocity vs. Sample Size	13
Figure 9	Power vs. Velocity	17
Figure 10	Power vs. Velocity	18
Figure 11	PPI plot (unfiltered)	19
Figure 12	PPI plot (GMAP)	20
Figure 13	PPI plot (Difference)	21
Figure 14	Range ambiguity	23
Figure 15	Reflectivity RHI plot (VH mode)	29
Figure 16	Reflectivity RHI plot (VHS mode)	30
Figure 17	Reflectivity RHI plot (Random coding)	31
Figure 18	Reflectivity RHI plot (SZ coding)	32
Figure 19	Scatter plot of average powers (VH mode vs. VH mode)	33
Figure 20	Scatter plot of average powers (VH mode vs. VHS mode)	34
Figure 21	Scatter plot of average powers (VH mode vs. Random coding)	35
Figure 22	Scatter plot of average powers (VH mode vs. SZ coding)	36
Figure 23	Estimation error of clustering algorithm	41
Figure 24	Comparison of CRT and clustering algorithms	42

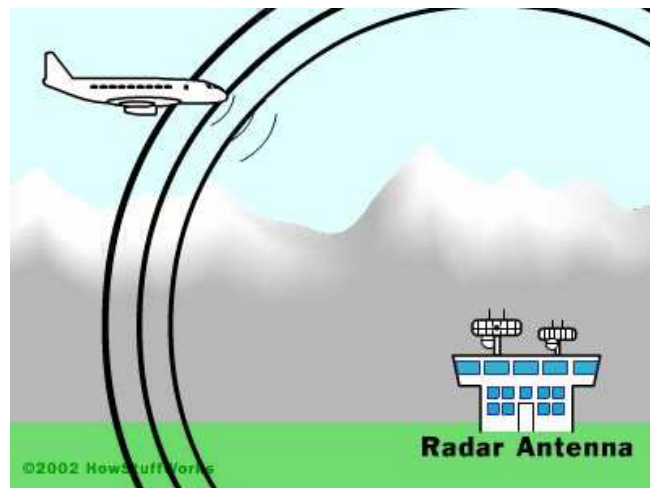
LIST OF TABLES

Table 1	Phase coding analysis summary	36
---------	-------------------------------	----

1 Introduction

Radar systems today have many different uses. This includes applications in weather, military, and civilian areas. This project focuses on the use of radar in weather applications, as used by CSU's CHILL weather radar.

RADAR, as an acronym, stands for RAdio Detection And Ranging. The basic idea behind radar systems is to send out a signal and listen for an "echo" of this signal off of a target. The first experiments that lead to radar occurred in 1887 by Heinrich Hertz who experimented with wave propagation in air. These experiments led to Christian Huelsmeyer's public demonstration in 1904 by successfully detecting a ship in the nearby harbor. During World War II, there was extensive research performed by American and British agencies, who eventually combined efforts to improve upon existing radar technologies. Following the war, surplus radar systems were picked up for use by other agencies not affiliated with the military, which led to the eventual discovery of Doppler radar systems in 1958. Today, radar is used extensively in applications beyond military, including weather detection.



(Figure 1)

In radar systems, there are two main types of targets – point targets and distributed targets. Point targets are more centralized in space (ie, airplanes), while distributed targets are less centralized (ie, weather patterns). There is a distinction between stationary targets (ie, buildings) versus moving targets (ie, cars), as well. If the target is moving, usage of the Doppler effect can determine how fast the object is traveling.

The Doppler effect, in a nutshell, is a noticeable frequency shift depending on the relative velocities of the target and the observer, usually given as:

$$f' = f_0 \frac{v + v_0}{v - v_s}$$

where f_0 is the initial frequency, v_0 is the velocity of the observer, and v_s is the velocity of the source. An example of this would be a passing police car, blaring its' sirens. As the car nears you, the pitch of the siren will seem to increase, and once it passes, it appears to drop in pitch. However, the siren's frequency didn't change at all. This phenomenon is useful in radar systems, specifically Doppler radar systems. However, for weather radar, the shift in reflected frequency is very, very small, and thus hard to detect. In this case, there is actually a very large shift in the phase of the returned signal in relation to the transmitted wave. By using this idea, we can relate the Doppler effect to phase by realizing that:

$$v(\theta) = \frac{\Delta\theta c PRF}{4\pi f}$$

where $\Delta\theta$ is the difference in phase between the received and transmitted signals, c is the speed of light, and f is the operating frequency of the radar transmitter. The PRF of a radar system only relates to a pulsed-Doppler radar system, as it is the rate at which pulses from the radar are transmitted. The velocity is also able to be calculated in continuous wave systems, but our focus will be exclusively on the pulsed-Doppler radar systems. The signal itself can be modified with

different properties depending on the application used. CSU's CHILL radar is a pulsed Doppler radar.

Some newer pulsed-Doppler radar systems are researching the use of dual wave polarization. By broadcasting a horizontally polarized wave, followed by a vertical polarized wave, reflected signals can be compared to better understand the shape of the target. CSU's CHILL is currently doing research in these dual polarization techniques.

Some inherent problems with radar detection are clutter, range ambiguity, and velocity ambiguity. Clutter refers to noise received by the radar in addition to reflected signals. This noise can come from anything (usually stationary objects), as we witnessed during our visit to CHILL. Jim George pointed the radar towards the highway, not transmitting anything, and showed us the noise created just by passing cars. Another type of clutter is from stationary objects such as the ground or buildings.

Range ambiguity is a situation in radar signal processing where received signals from different ranges appear to have the same range. The maximum range can be determined by the following:

$$r_{\max} = \frac{c \cdot T}{2}$$

where T is the pulse repetition period (which is the inverse of the PRF). The maximum range can be increased by decreasing the PRF, but this also decreases the maximum velocity that can be detected without ambiguity.

Velocity ambiguity is a problem in radar data processing where received signals from different velocities have a phase shift of greater than 2π , thus overlapping and giving false velocity readings. The maximum velocity can be determined by:

$$V_{\max} = \frac{\lambda}{4T}$$

where λ is the wavelength of the transmitted signal. As you can see, from the two equations above, there is a tradeoff between maximum range and velocity, as seen below:

$$r_{\max} \cdot v_{\max} = \frac{c\lambda}{8}$$

We will be discussing techniques to address these issues, both currently practiced and theoretical, later in the paper as researched throughout both semesters. Data from CSU-CHILL radar and CASA radar systems, as well as computer simulations, were used to research and implement these solutions.

2 Simulation Results

After learning about the basics of radar, we began to run some simulations in Matlab to get some experience with the data processing of radar signals. Our first simulation was to simulate a radar signal with and without clutter. After simulating these results, we plotted them using a variety of windows, including rectangular, Hamming, and Blackman windows. The use of a variety of windows is important to accurately interpret radar data. Below are figures of our simulations of radar data with clutter (in blue) and without clutter (in red) using three different windows.

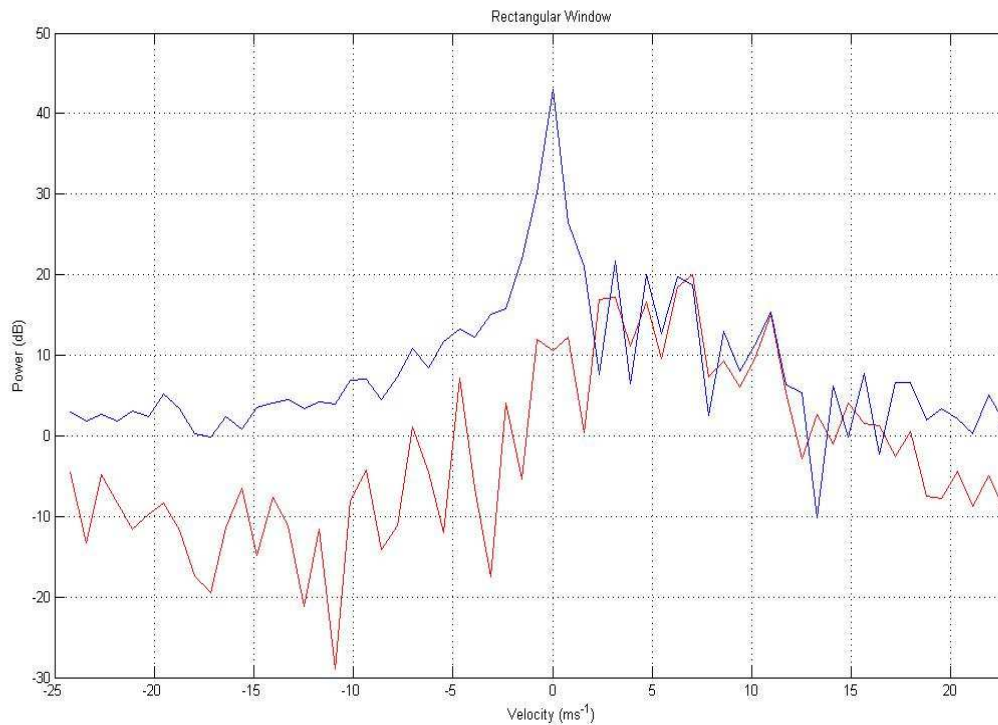


(Figure 2)

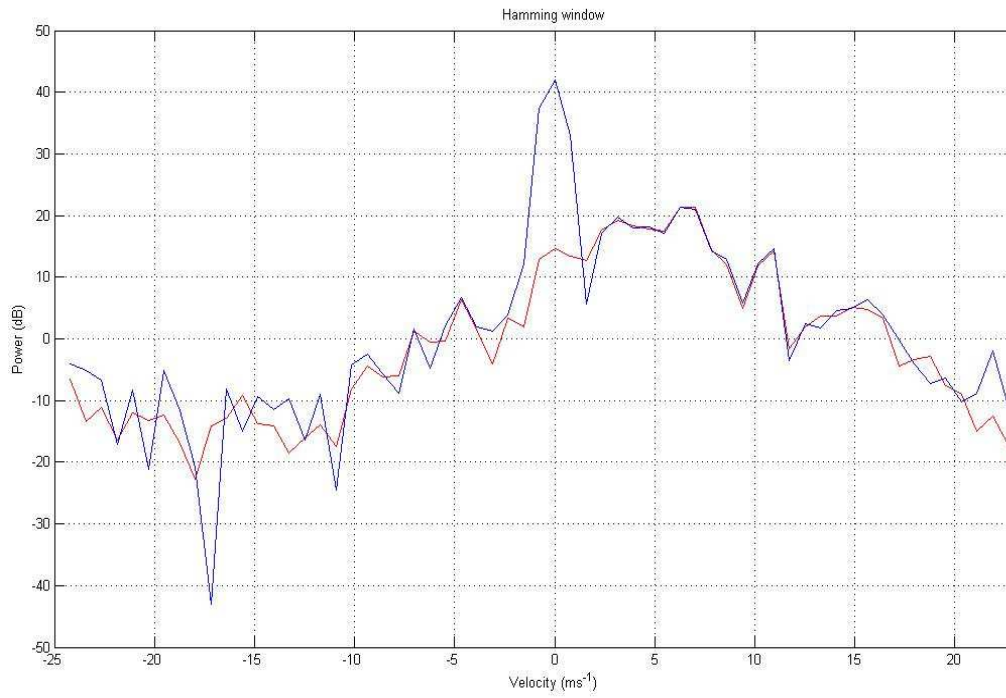


(Figure 3)

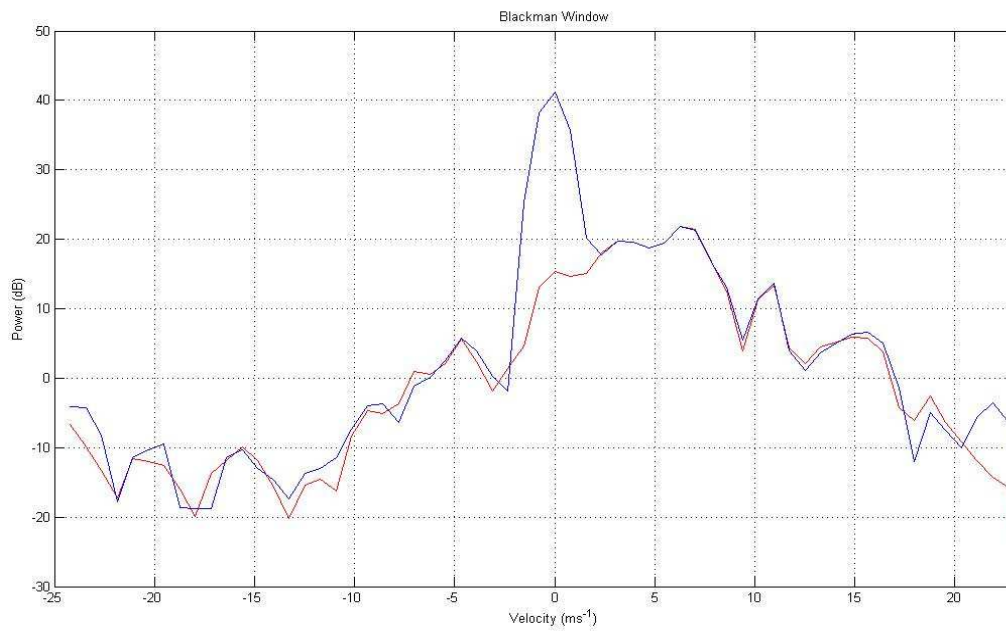


(Figure 4)

Since a rectangular window has a relatively small width for the main lobe in the frequency domain (compared to a Hamming or Blackman window), there are sharper peaks.

Since Blackman and Hamming windows have a larger main lobe width, these windows result in smoother results (as seen above). Also, since the side lobes of a rectangular window are relatively large (approximately -13 dB for peak side lobe), clutter will affect the total signal more than the Blackman or Hamming windows (approximately -57 dB and -41 dB, respectively). See Appendix A for details on Matlab code used for this simulation.

Our next simulation involved altering the number of samples used and viewing the effects on power and velocity calculations. Specifically, we determined the mean and standard deviation of power and velocity for sample sizes of 16 to 256 with a step size of 16. Below are the generated simulation results.

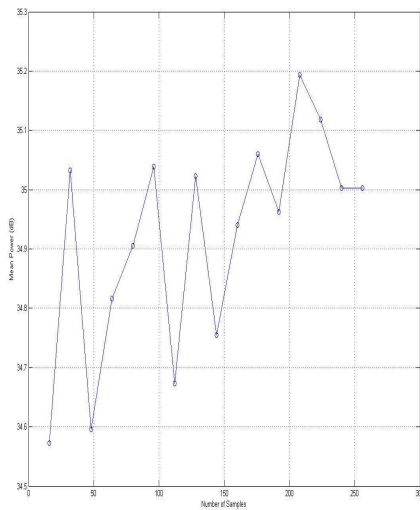


(Figure 5)

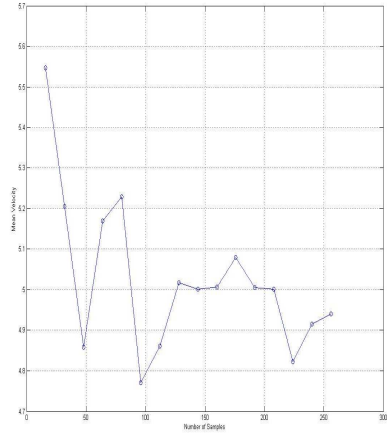


(Figure 6)

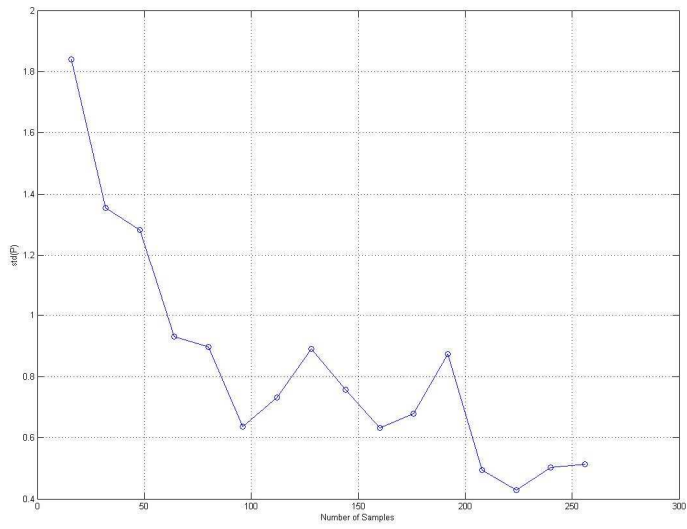


(Figure 7)

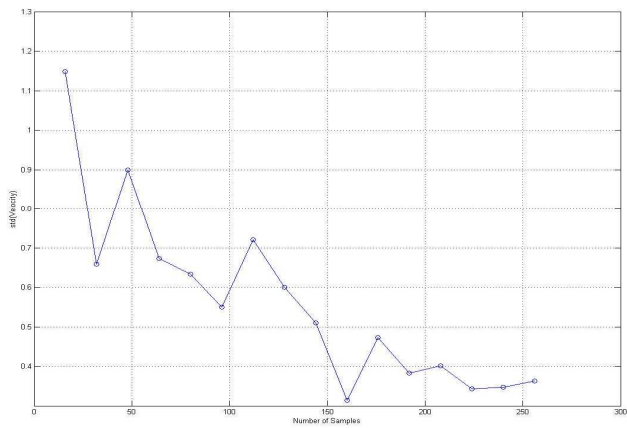


(Figure 8)

As seen above, as the sample size increases, the accuracy of the mean power and mean velocity increases. Additionally, as the sample size increases, the standard deviation of power and velocity decreases. These results matched our predictions of how sample size should affect these parameters. Appendix A contains Matlab code for this simulation.

Now that we've simulated radar signals and have an understanding of various calculations performed on simulated received data, we can begin to analyze our specific problems – clutter, range ambiguity, and velocity ambiguity.

3 Clutter

3.1 Overview

Clutter is unwanted radar echo. These echoes can “clutter” the radar output and make it hard to detect wanted targets. In particular, ground clutter is undesired radar echoes that come from the ground. Ground clutter is difficult to quantify and classify since radar echoes from land depends on many variables that need to be considered before doing anything. Getting rid of clutter or compensating for the loss caused by clutter might be possible by applying appropriate filtering and enhancing techniques [2].

In the past, most weather radar processors have been built using the approach of a fixed notch-width infinite impulse response (IIR) clutter filter followed by time-domain autocorrelation processing called pulse pair modulation. Although this method was widely used there were many drawbacks in using this clutter filtration method. The impulse response of an IIR filter acts just like it sounds, infinite. This means that any perturbations that are encountered, such as a very large point clutter target or change in the pulse repetition frequency (PRF), will affect the filter output for many pulses, sometimes affecting the output for several beam widths. The use of clearing pulses or filter initialization can diminish its effect at the cost of reducing the number of pulses. Another problem is that the filter width used to remove the clutter depends on the strength of the clutter. If the strength of the clutter is very strong then a wider filter must be used. This would be problematic because the filter would either be not aggressive enough for strong clutter or overly aggressive in removing weather echoes.

Others have approached the clutter problem by using fast Fourier transform (FFT) processing. The advantage of an FFT approach is that the ground clutter filtering can be made

adaptive by searching in the frequency domain to determine the boundary between the system noise level and the ground clutter. The FFT is just a frequency impulse response (FIR) block processing approach that does not have the same problems that the IIR filter has. Just like an IIR filter, the FFT approach has two distinct disadvantages. First, spectrum resolution is limited by the number of points in the FFT, which has the constraint that it must be a power of two.

Operational systems are normally either a 32 or 64 point FFT, so if the number of points is low, then clutter will be spread over a bigger part of the Nyquist domain which can obscure weather targets [1]. The second disadvantage is when a time-domain window is applied to the in-phase I and quadrature-phase Q (IQ) components of the echo prior to performing the FFT in order to get the best performance. The drawback of using windows is that they reduce the number of samples that are processed, which will make the estimates have a higher variance.

The Gaussian model adaptive processing (GMAP) provides many advantages over pulse-air processing with fixed IIR or FIR filters. GMAP is a frequency domain approach that uses a Gaussian clutter model to remove ground clutter over a variable number of spectral components that is dependent on the assumed clutter width, signal power, Nyquist interval, and number of samples. The GMAP approach makes certain assumptions about clutter, weather, and noise. These assumptions include the weather signal's spectrum width is greater than that of the clutter, the Doppler spectrum consists of ground clutter, there is only a single weather target and noise, the width of the clutter is approximately known, and the shape of the clutter and weather is a Gaussian. The way that GMAP works is by applying a Hamming window to the IQ values and then a discrete Fourier transform (DFT) is then performed. The Hamming window is used as the first guess - after analysis is complete, a decision is made to either accept the results or use a more aggressive window based on the clutter to signal ratio (CSR). Next, the power in the three

central spectrum components is summed and compared to the three central components of a normalized Gaussian spectrum. The Gaussian is extended down and all spectral components that fall within the Gaussian curve are removed. Once all the components are removed, a Gaussian is fitted to fill in the clutter points that were removed. This step is repeated until the computed power does not change more than .2dB and the velocity does not change by more than .5% of the Nyquist velocity. Finally, GMAP determines the optimal window based on the values of the clutter to signal values.

3.2 Solution Researched

In order to understand GMAP better, for our second semester we began by trying to figure how to effectively use GMAP on data received from CASA and LAWTON radar. We first figured out how to get GMAP to work on simulated data that we had used from the first semester when we added ground clutter to the signal seen in figures 4. We then applied GMAP to the data to see the effectiveness of the clutter filtering done by GMAP. As seen below, we can see that the original signal generated and generated clutter around zero velocity. The Black line shows that GMAP effectively removes the signal that is ground clutter and models it to a Gaussian and the rest of the signal. In the figure it also shows that the signal that is below the noise floor is also removed.

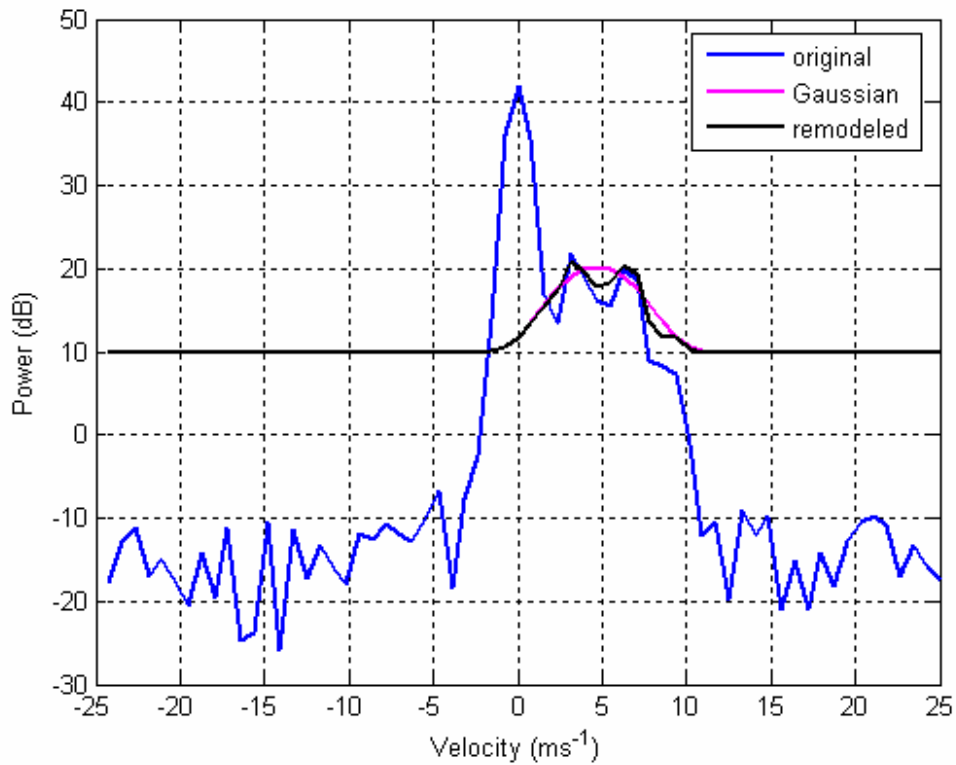


(Figure 9)

The next step that we took was to see how effective GMAP would be with data received from CASA radar. The problem with getting this data was converting the raw data into a form that we could use in order to find the effectiveness of GMAP. To do this we used Matlab to convert the raw data into a time series to find estimations for the velocity and power. From the power we were able to get the reflectivity of the received data. Seen below is a plot of the raw data received from LAWTON radar on the 13th of March at 2:29 of power versus velocity.

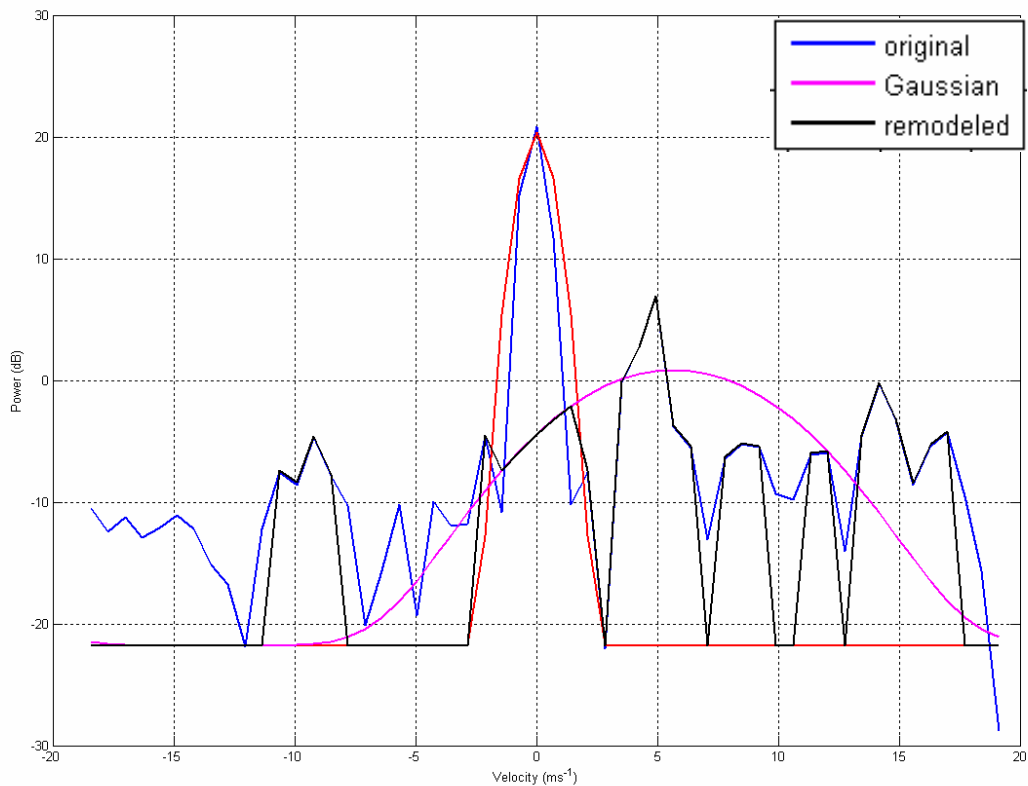


(Figure 10)

We can see here again that effect of GMAP works pretty well with the data received from the radar we can see that it takes about 20 dB of clutter out from the signal and replaces it with a Gaussian.

The next step that we took was to take our findings and apply it on a larger scale to see how much GMAP would help with data received from LAWTON radar. To do this we had to understand how the radar collected the data. We found out that when a signal is sent out the radar starts at a certain azimuth degree and a signal is sent out. The signal is broken into 700 gates and each gate is sampled 54 times the number of gate and samples depend on how the user wants to receive the signal. Then the azimuth degree is changed and the same process is done

again. From there the raw data is saved for the user to do research. In order for us to see the effects of GMAP on LAWTON radar we had to apply GMAP to each gate of every azimuth degree. Below is the result from the radar turning 360 degree on March 13, 2007 at 2:29pm with no filtering.

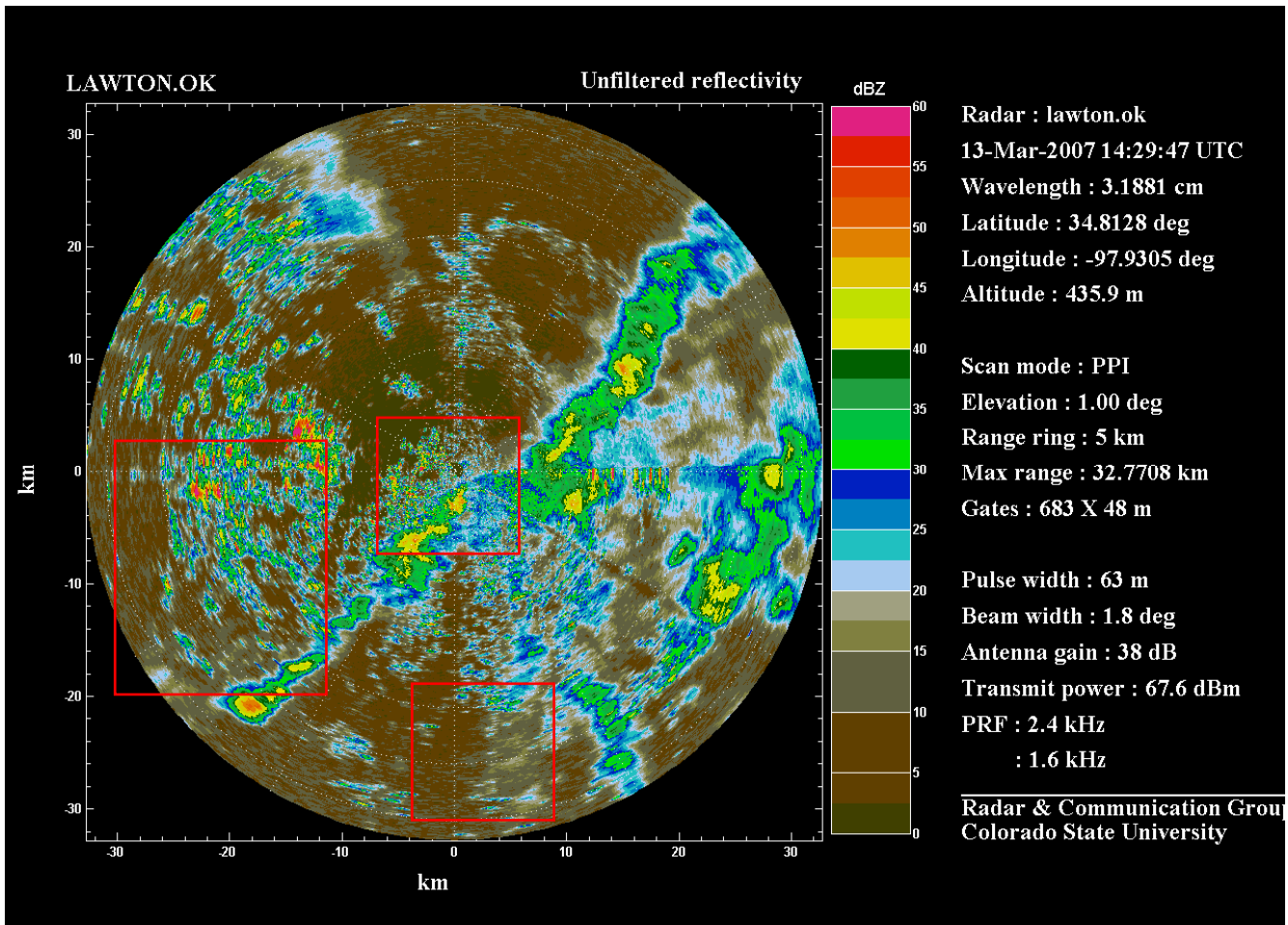


(Figure 11)

In the figure above is a reflectivity plot of the weather we can see that there is a lot ground clutter in the selected areas. But with GMAP filtering we can see that it takes a lot of this clutter is taken out so that better models of this weather can be taken. The figure blow is the same data taken from LAWTON radar but GMAP filtering is applied to the signal.

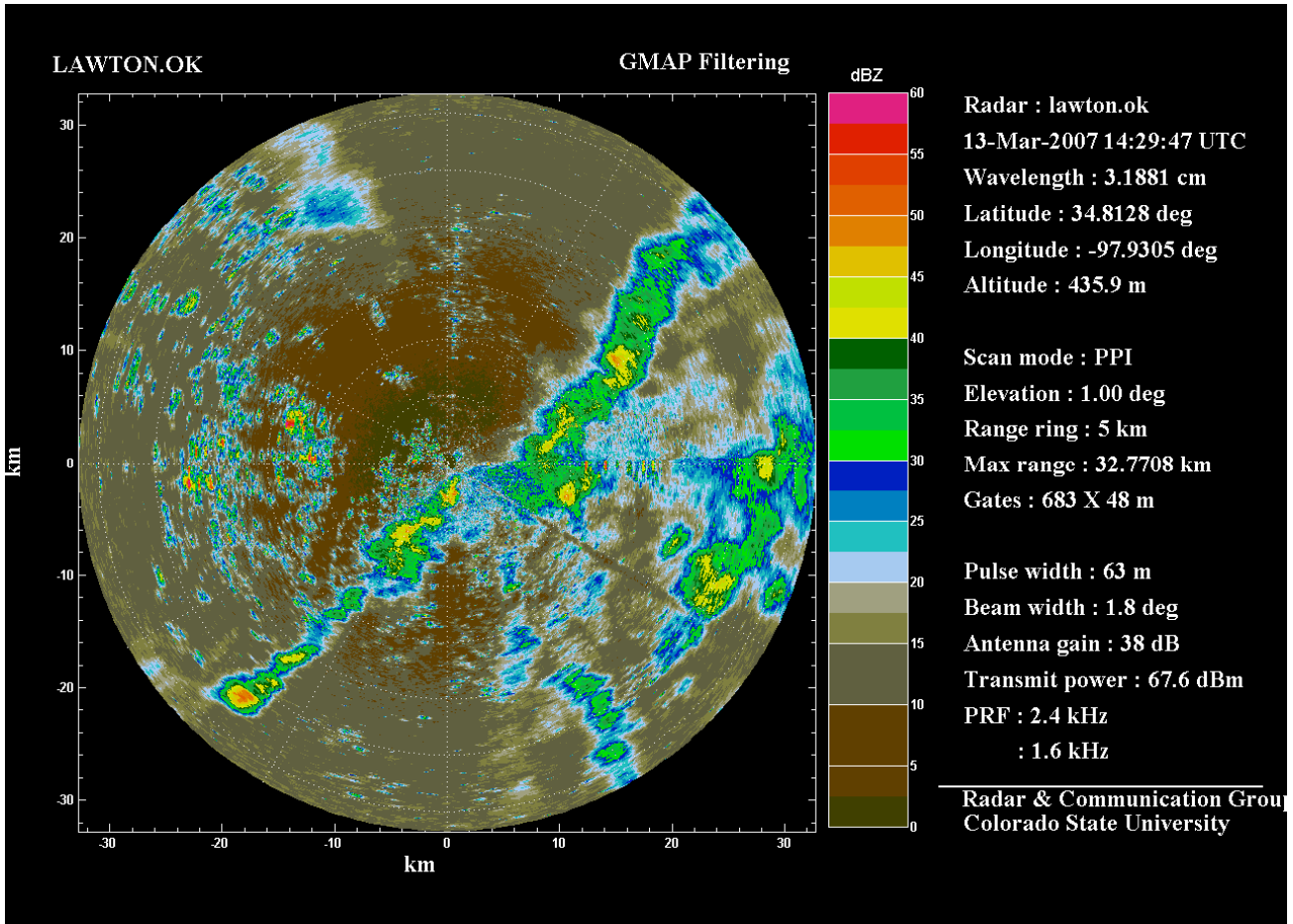


(Figure 12)

We can see that in the areas that were highlighted from above that a lot of it is removed from the figure and what is left is mostly from the weather. Showing how effective GMAP can be at removing ground clutter. In order to demonstrate how much clutter is removed we also plotted the difference of the figure 11 and figure 12 to show the removed power that GMAP actually did in the plot seen below.

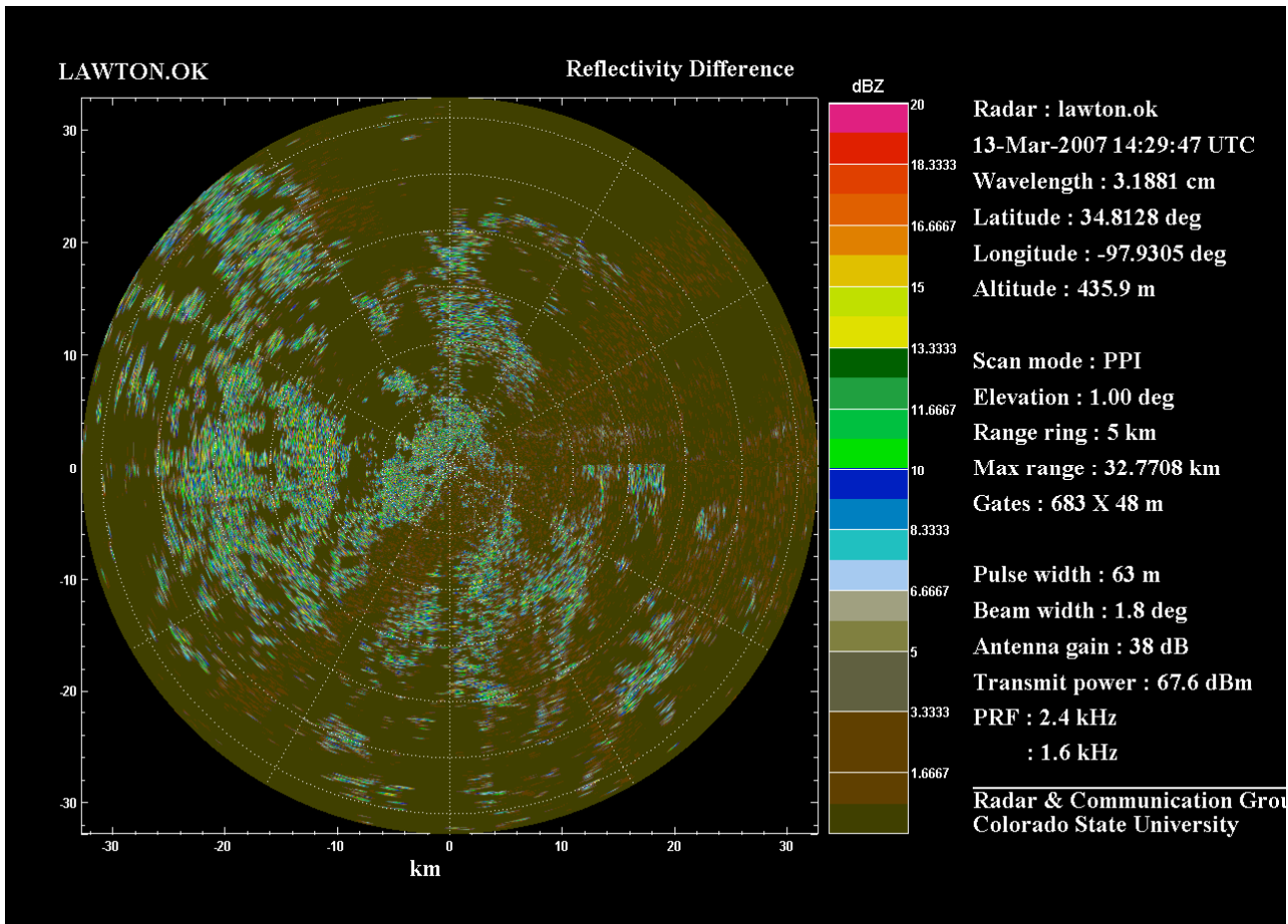


(Figure13)

We can see here in this figure that on average GMAP mostly took out around 11.5 dB- 13.33 dB of ground clutter from the received signal. Although GMAP doesn't take out all the Ground clutter we can see how it helps with only keeping the signal from the weather target.

3.3 Conclusion and Future Work

Based on what we can see from these figures we can see that GMAP is good at taking out the unwanted ground clutter but we still see that there is some ground clutter left in the figures. We can also see that GMAP is an adaptive filtering technique that is effective in removing the ground clutter. Future work can be done by running more data sets to see the true effectiveness of ground clutter or to see if there is an even better way to remove ground clutter that distorts wanted signal received by radar.

4 Range Ambiguity

4.1 Overview

Range ambiguity is a situation in radar signal processing where received signals from different ranges appear to have the same range. When a pulse is sent from the radar, it must travel, hit an object, and return before the next pulse is sent to avoid range ambiguity. When a pulse is sent and a reflection is not received before the next pulse, an ambiguity in range occurs as illustrated below.

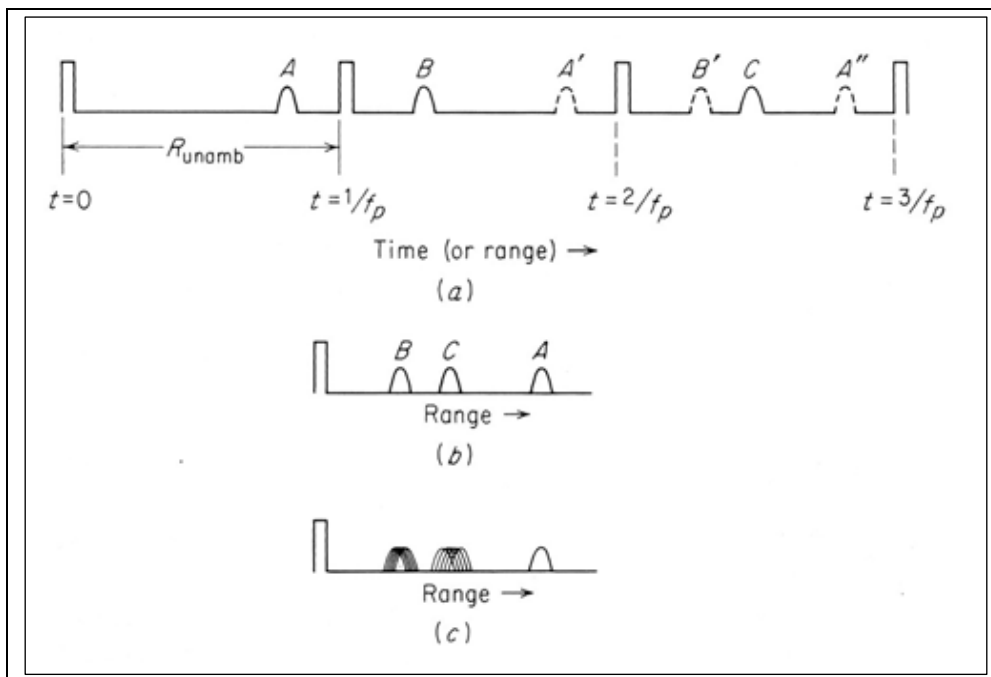


(Figure 14)

As seen above, target B appears to be closer than target A, when in fact, target A is closer than target B.

The maximum range can be determined by multiplying the period of the PRF by the speed of light (speed of propagating waves) and dividing by two to account for a roundtrip.

Below is the general relationship between maximum range and the period of the pulse repetition frequency.

$$r_{\max} = \frac{c \cdot T}{2}$$

As seen above, maximum range is directly related to the period of the PRF and inversely related to the PRF. Allowing the period of the PRF to become very large will increase the maximum range, but will introduce greater velocity ambiguity. As a result, there is a trade off between range and velocity ambiguities when processing data from radars. Depending on the application of the data, one of the two measurements may be more important. Typically, MTI (moving target indicator) radars operate with unambiguous range measurements, but with ambiguous velocity measurements [2]. Pulsed Doppler radars tend to operate with unambiguous Doppler measurements, while having ambiguous range measurements. In our studies, weather data received by the CHILL radar needs to have strong measurements in range and velocity to accurately model weather patterns. Velocity ambiguity will be discussed more in depth later in the chapter.

Techniques have been devised to lower the effects of range ambiguity including a technique called “phase coding”. Phase coding alters the phase of the radar signal before transmission in an attempt to reduce range ambiguities. This phase difference, a_k , is determined by a value Ψ_k , which is determined by the type of phase coding.

$$a_k = \exp(j\psi_k)$$

Phase coding consists of an encoding and a decoding state. In the encoding stage, the signal to be transmitted is multiplied by the phase offset, a_k . The next signal received is then multiplied by a_k^* . If the signal is a first trip signal, then this will make the signal coherent. If, however, the signal is a second trip signal (it was originally multiplied by a_{k-1}), then it will now

be phase modulated by $c_k = a_{k-1} a_k^*$. We will be considering only first and second round trip signals, as this technique can be extended to compensate for further order trips. Additionally, we will consider the first round trip signal to have greater power than the second round trip.

Analysis is nearly the same if the opposite is true. Now, depending on the type of code used, one is able to alter the spectra of the two signals. However, before individual codes are examined, a few useful properties of codes will be examined.

Given the situation where a first round trip and a second round trip signal are overlaid, it is helpful if the autocorrelation at lag T is equal to zero (ie, $R(1) = 0$). Since velocity can be calculated by finding the $\arg[R(1)]$, the velocity of the first signal can be calculated without interference from the second signal (as it will have lag T and thus zero autocorrelation). A second useful property when designing codes is the capability to reconstruct signal spectrum from a small part of the original spectrum. This is useful because some filtering of the first signal may occur before the second signal's spectrum is reproduced. Types of codes will now be examined.

The first types of phase coding introduced were systematic phase coding and random phase coding. In a systematic phase coding procedure, the phase difference between successive pulses is uniform. An example of this is using a phase offset of 0 on the first transmitted pulse, a phase offset of $\pi/4$ on the second pulse, and a phase offset of $\pi/2$ on the third pulse. This is the most intuitive type of phase coding, but another type of phase coding was introduced called random phase coding. Depending on the application, random phase coding may be superior to systematic phase coding. Random phase coding simply uses a phase offset that is random between pulses.

A new type of phase coding was developed in recent years called SZ coding developed by M. Sachidananda and D. Zrnic [3]. In this type of phase coding, the phase offset is determined by the number of samples M and a factor n to be chosen, which will affect the period of the code. Below is the formula determining the phase offset in this code.

$$\varphi_{(k)} = \psi_{(k-1)} - \psi_{(k)} = n \pi k^2 / M$$

For example, the SZ(8/64) code, has 64 samples and repeats every 8th sample. The SZ code was constructed to have the two properties discussed above: autocorrelation at lag T equals zero and possible spectrum reconstruction from a small portion of the original spectrum. In the case of the SZ(8/64) code, autocorrelation is one at lags of 8, 16...64 and autocorrelation is zero at all other lags. From this property, one can effectively calculate velocity estimates on the first signal without error from the second signal. Once the velocity of the first signal is determined, a notch filter around this velocity can be implemented on the complete signal spectrum. From the resulting signal, the velocity of the second trip signal can be estimated. Simulations conducted by Sachidananda and Zrnic have shown this technique to be superior to random phase coding and systematic phase coding. Velocity ambiguity and techniques to reduce the effects of velocity ambiguity will now be examined.

4.2 Solution Researched

In the second semester of this project, real radar data was collected using different coding schemes. Using the CHILL radar on December 28, 2006, different coding techniques were utilized on data collected from a snowstorm around 11:54 PM. There were two intended goals when analyzing the data. The first goal was to determine if there were second trip signals

present and the second goal (if there were second trip signals present) was to analyze the effectiveness of the coding techniques to suppress second trip signals.

To effectively compare the coding techniques, data was collected in VH and VHS mode without coding. VH mode switches polarizations between subsequent pulses, while VHS mode broadcasts both polarizations on all pulses. Since VH mode will effectively have twice the range of VHS mode, VH mode can be used a standard for determining if second trip signals are present.

Using VH mode with no coding as a standard to compare other coding techniques, different metrics were needed to effectively compare the results. Two such metrics were used: comparison of reflectivity (dBZ) plots and comparison of mean velocity plots. First, reflectivity will be introduced.

Reflectivity is a measure of the energy being reflected by a given target. It is measured using units called dBZ and is calculated using the formula below.

$$Z(\text{dBZ}) := P(\text{dB}) + G_r + C + 20 \cdot \log(r)$$

where Z = reflectivity in dBZ, P = received power in dB, G_r = receiver gain, C = radar constant, and r = range in km. Reflectivity is important in analyzing radar, as it can be an indication of the type of precipitation (if one is present). Values of 40+ dBZ indicate rain with higher values indicating heavier rain and values of 30 – 40 dBZ indicate snowy conditions. Since data collected on December 28, 2006 was during a snowstorm, it was expected that data collected would be in the range of 30 – 40 dBZ. Below is reflectivity in VH mode using a RHI (row height indicator) plot.

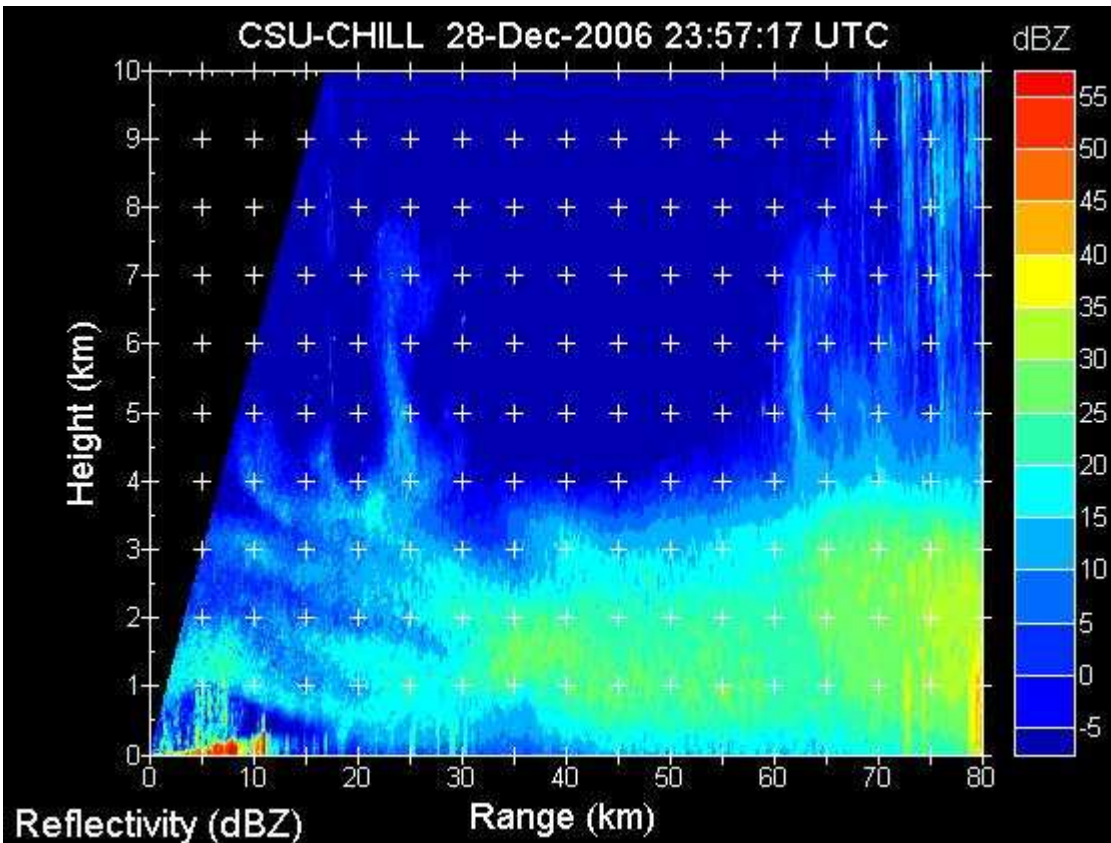


(Figure 15)

As seen above, data in the range of 40 – 80 km has a reflectivity value between 15 and 35 indicating a snowstorm is occurring. This plot corroborates with the physical conditions that were present on December 28th. A few distinct characteristics can also be seen in the above plot. First, precipitation is occurring below a height of 4 km. This is where precipitation is expected to occur. Second, ground clutter near the radar can be seen between 0 and 10 km near the ground. Finally, the storm appears to be strongest at 80 km (with a reflectivity value of approximately 35 dBZ). This reflectivity plot in VH mode is used as the standard for comparing other coding techniques.

The first coding technique compared is VHS mode with no coding. This is the situation where the energy being sent is dual polarized, but is not phase coded in any way. Below is a

reflectivity plot in VHS mode.

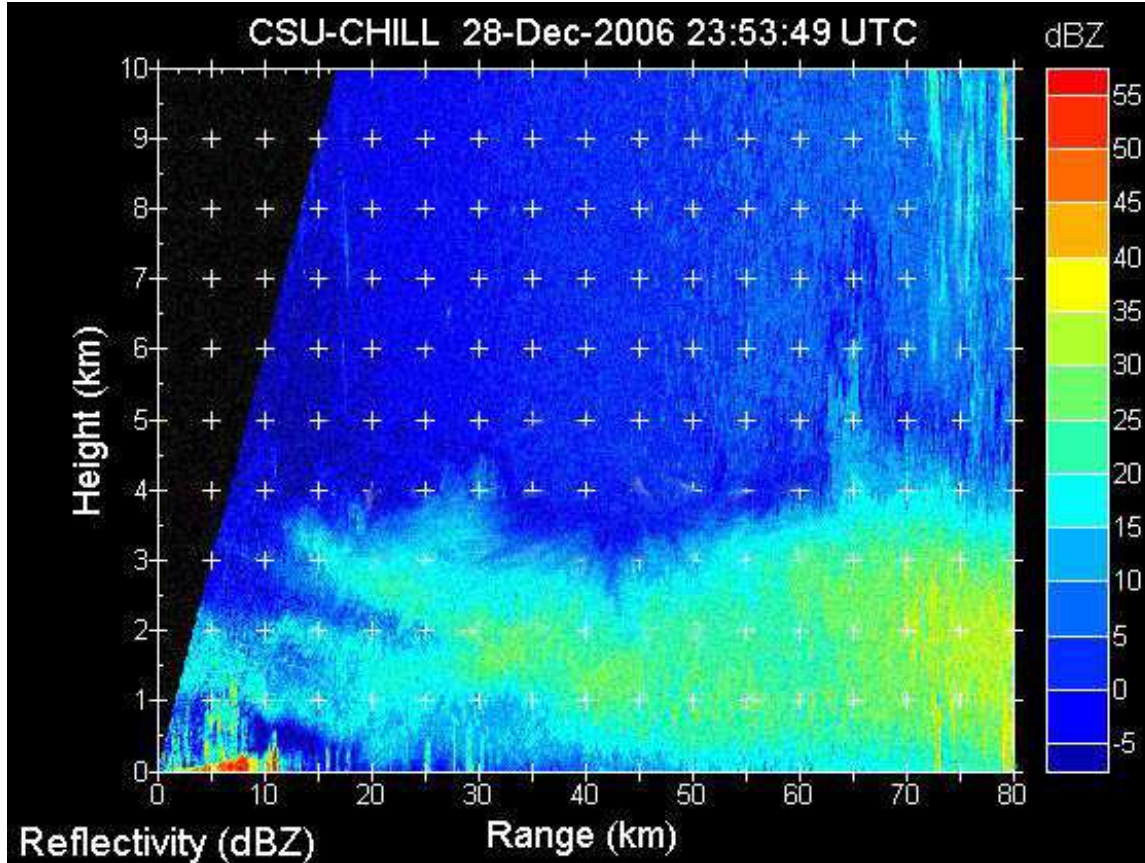


(Figure 16)

Seen above, the data collected in VHS mode is different than the data collected in VH mode, though the differences appear to be minute. One specific area where reflectivity measurements differed was at a range of 20 km and a height of 4-6 km. The VH mode reflectivity plot shows values of 10-20 dBZ in this area, while the measurements are less than 0 dBZ in the VHS mode. Overall, however, differences between the plots seem to be very small.

Next, random phase coding was analyzed by attaching a random phase component to dual polarized signals before they were to be analyzed. Upon their retrievals, the signal would be made coherent by adding the complex conjugate of the original random phase. Below is a reflectivity plot of the random phase coding.

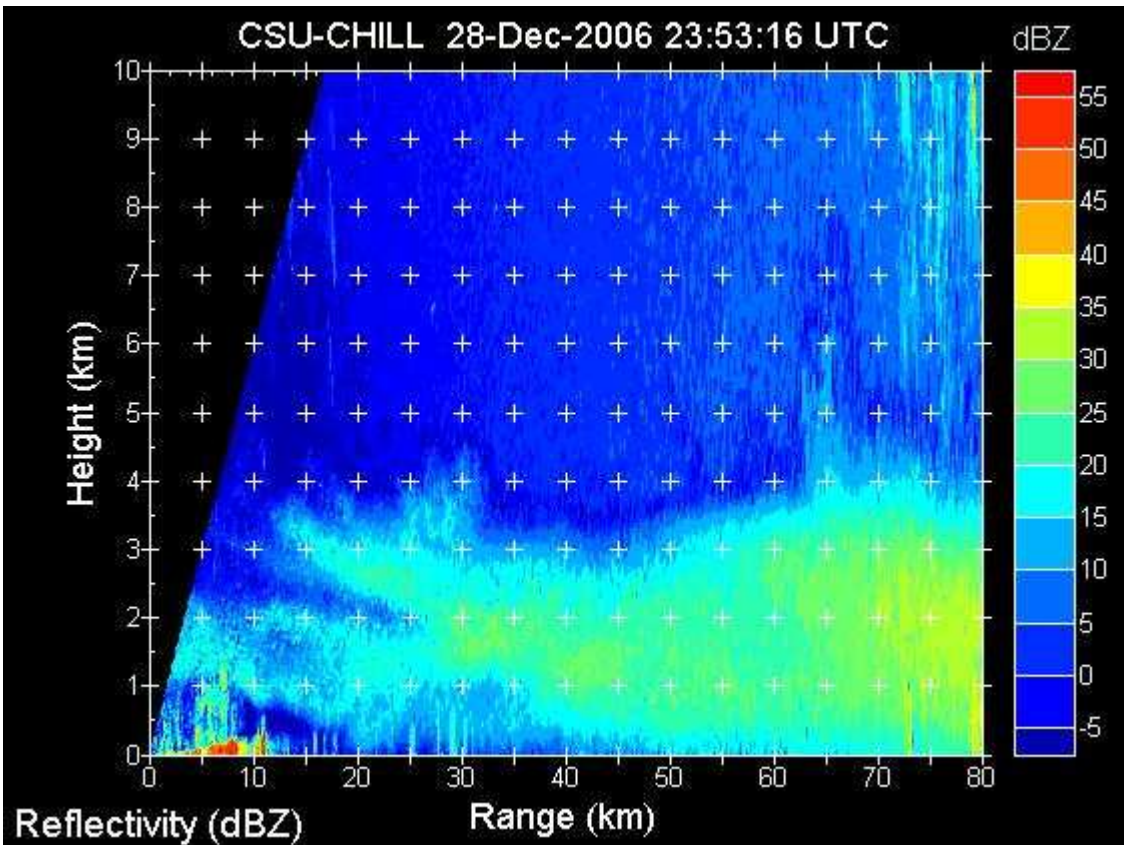


(Figure 17)

Random phase coding appears to be most similar to the VHS mode (which is expected), but generally, pretty similar to the VH mode. This result either implies that random coding is ineffective in this study or there are not second trip signals present. Before these questions are analyzed, SZ coding will be studied.

As described earlier, SZ coding is believed to far exceed the effectiveness of random phase coding, based on simulations. In this study, we examined how effective it was in real data collected by the CHILL radar. Below is the reflectivity plot of SZ coding.

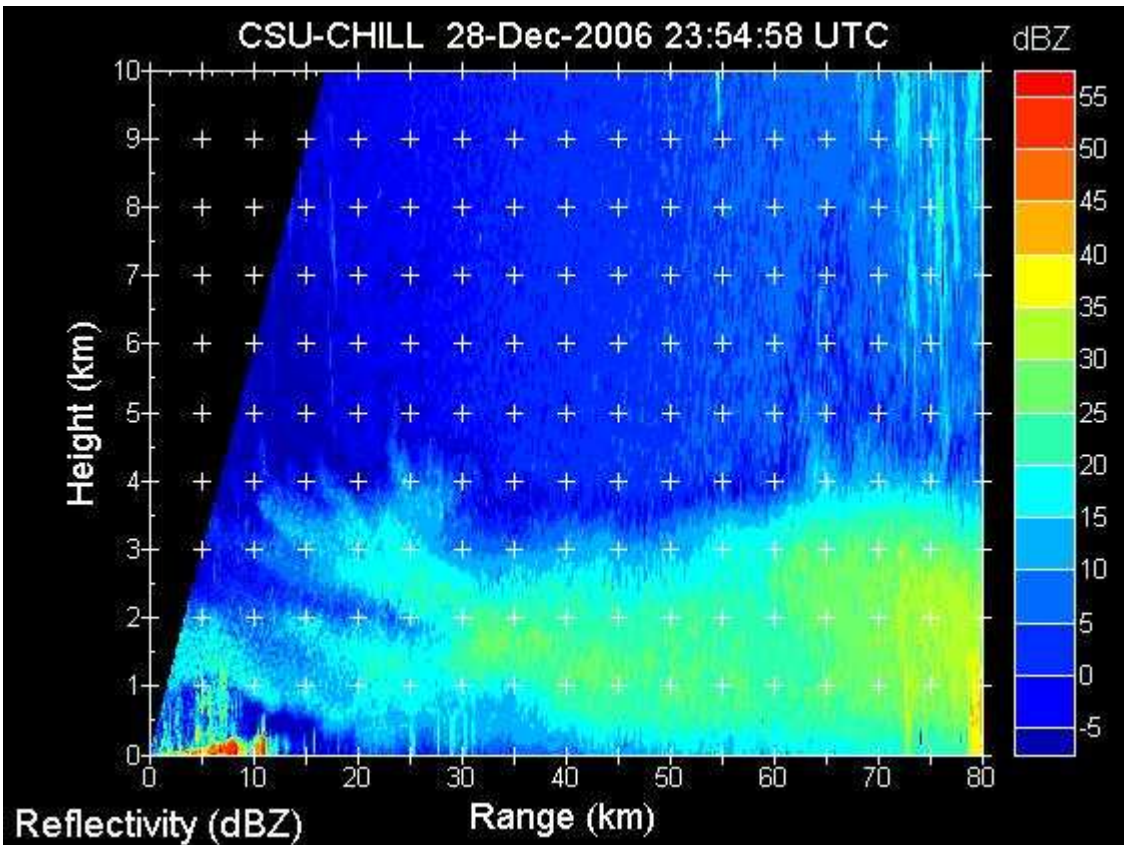


(Figure 18)

Again, SZ coding appears to be very similar to the earlier plots with its greatest similarity to random coding and the no coding (VHS mode) plots.

Based on reflectivity metric, it appears that few (if any) second trip signals are distorting the received data. This can be seen, as the data in VH mode and VHS mode appear to be very similar. There are some notable differences in the plots, but they seem to be inconsequential. Next, a different metric using average power was applied to help justify the previous conclusions.

Average power (in dB) at different ranges was calculated in VH mode and compared to similar measurements for the different coding techniques. Before this was completed, data collected for two different sweeps in VH mode were plotted for comparison and shown below.

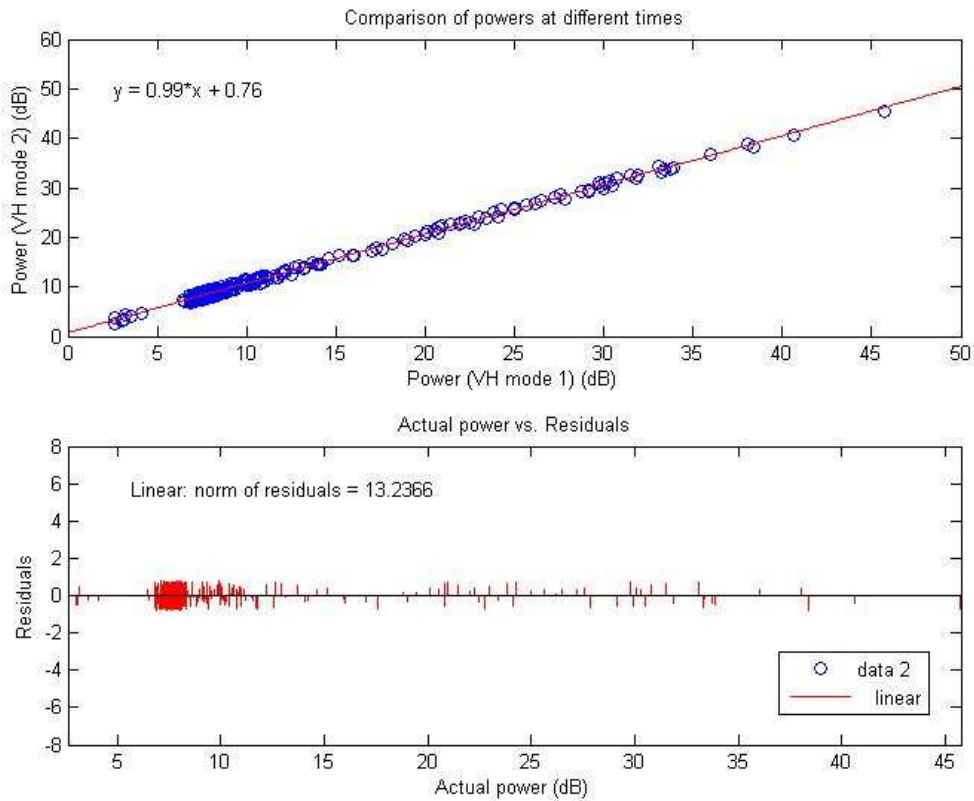


(Figure 19)

The first plot shows a scatter plot of the mean power at different ranges for the data collected in the first sweep of VH mode versus data collected in the second sweep of VH mode. Linear regression was completed on this scatter plot and was shown to be $.99x+.76$. Ideally, if the measurements were exactly the same, then the slope of best fit would equal 1, but in our case, $.99$ seems more than satisfactory for justifying the use of this metric. Additionally, the mean square error (norm of the residuals) was found to be equal to 13.2366.

The first coding scheme analyzed using this metric was the VHS mode (no coding) method and the results are seen below.

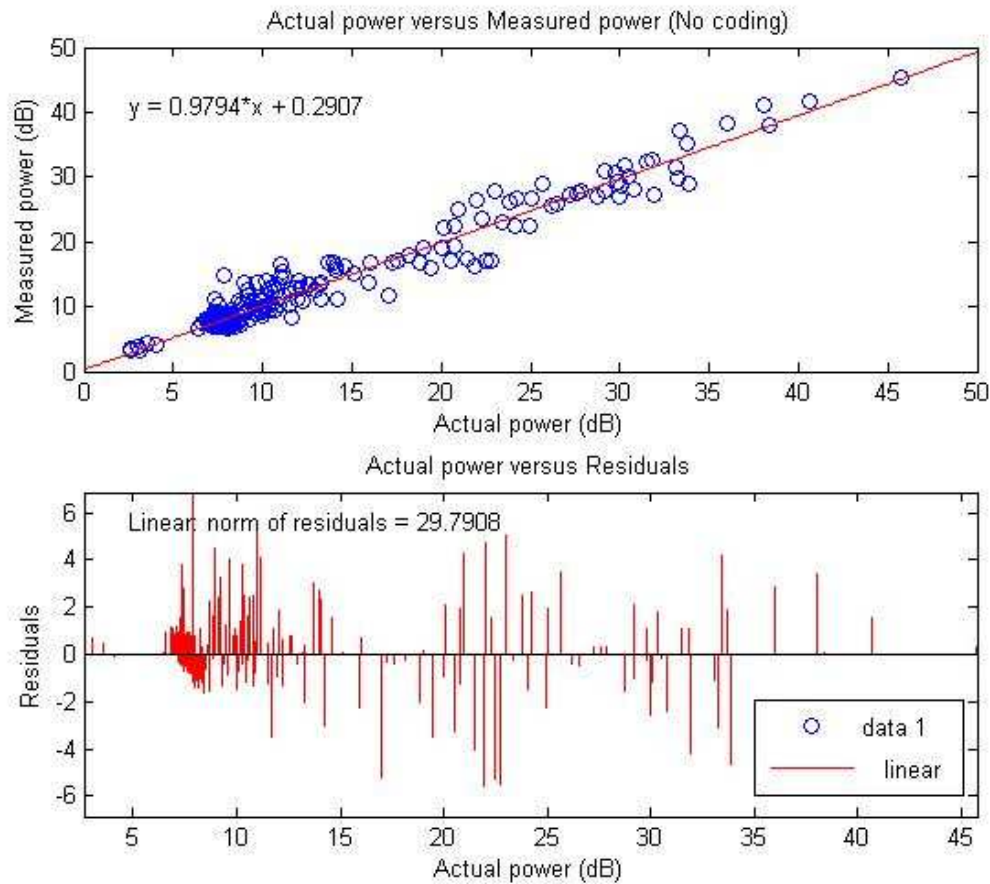


(Figure 20)

In the above plot, the slope is .97, which indicates not quite as good of correlation as the correlation between two VH mode sweeps. Additionally, mean square error was found to be 29.7908, which was far greater than the previous value of 13.2366. Next analyzed was the random coding scheme.

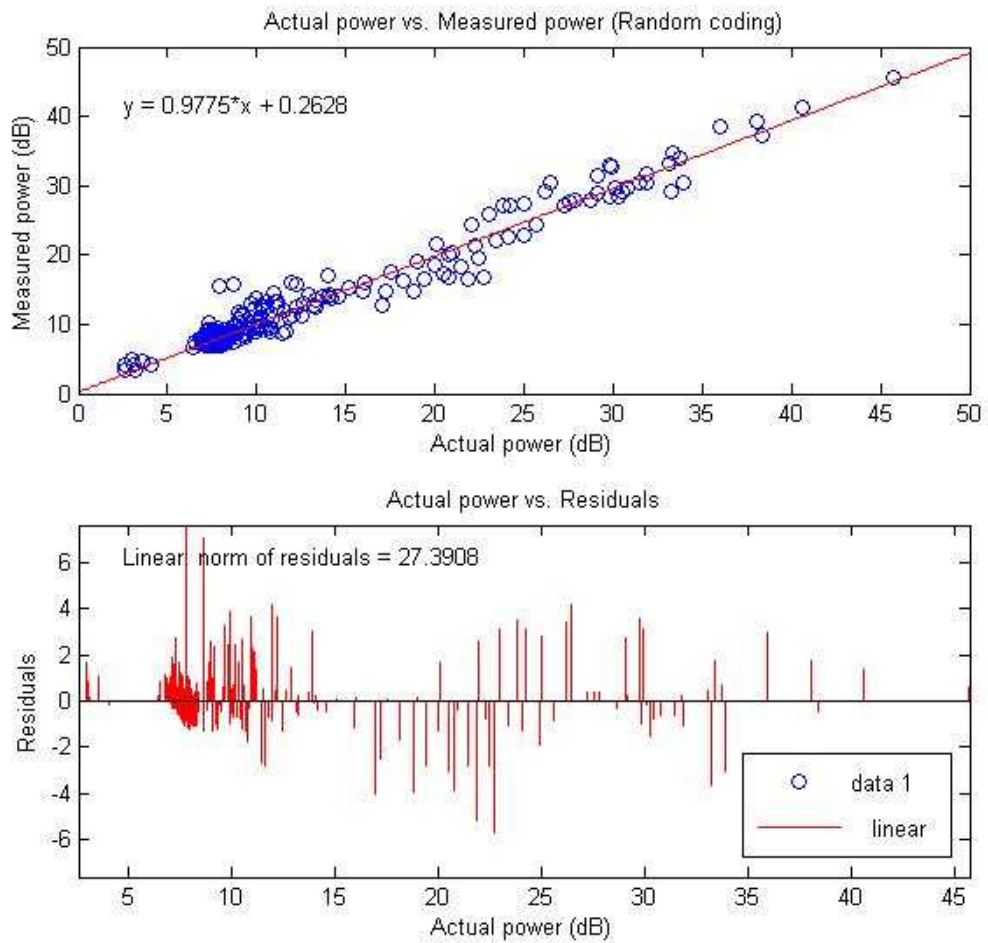


(Figure 21)

With the use of random coding, the slope calculated using linear regression was nearly identical to the value obtained in the case of no coding (.9775 for random, .9794 for no coding). The norm of the residues was smaller than the previous case with a value of 27.3908. Finally, SZ coding was analyzed using this metric.

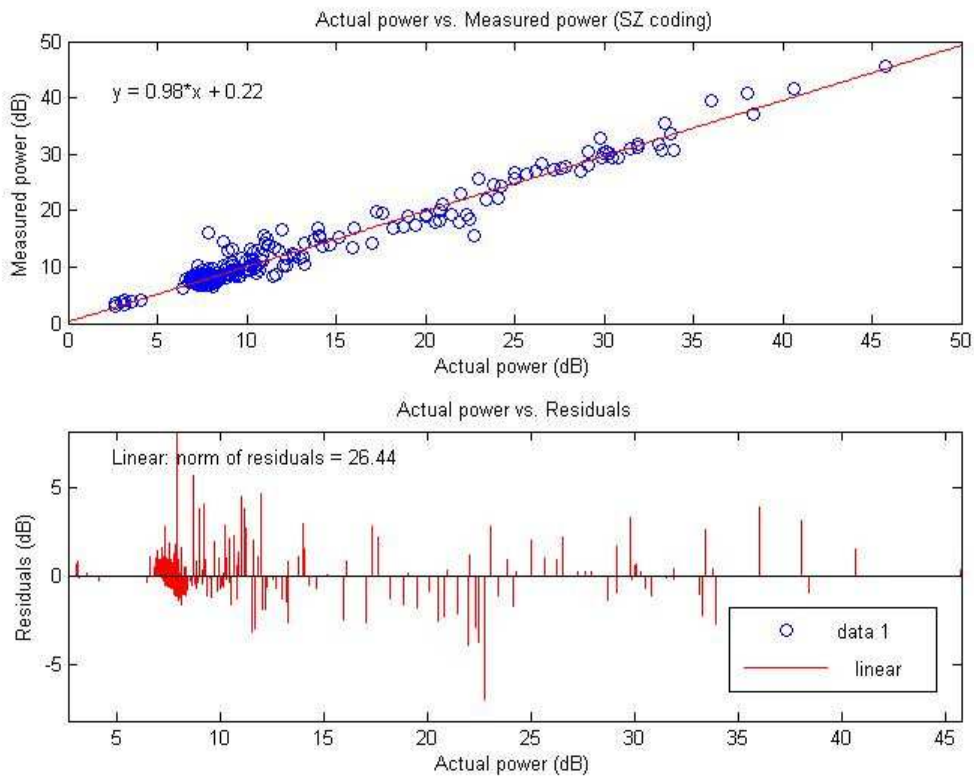


(Figure 22)

With the use of SZ coding, the slope of the scatter plot increased to .98 and the norm of the residues decreased to 26.44. Below the results are summarized in a table.

<u>Case</u>	<u>Slope of Best Fit</u>	<u>Norm of the residues</u>
VH mode vs. VH mode	.99	13.2366
VHS mode vs. VH mode	.9794	29.7908
Random coding vs. VH mode	.9775	27.3908
SZ coding vs. VH mode	.98	26.44

(Table 1)

Using the data provided above, clearly SZ coding outperforms random coding and no coding (VHS mode) techniques by minimizing the mean square error. The difference between the methods seems to be very small; however, implying the test was somewhat inconclusive.

4.3 Conclusion and Future work

Based on the two metrics, reflectivity and average power correlation, it was determined that second trip signals were either not present or too weak to exhibit an influence on the rest of the signal. This determination successfully completed the first objective of this section of the project: determine if second trip signals were present. The second objective was to determine the effectiveness of the different coding schemes (if second trip signals were present). This objective was null, as it was determined that second trip signals weren't present. Based on the data of the average power scatter plots, it appears that SZ coding slightly outperformed the other coding methods, but these results could be completely unsubstantiated since the differences were so small.

For future research into this topic, there are a few suggestions that are made for continuation of this project. First of all, the PRF should be increased substantially to increase the likelihood of second trip signals. Once it is determined that second trip signals are present, effective analysis of the different coding techniques could be completed. The second suggestion regarding future research is that many data sets are collected and analyzed to corroborate any initial results. The study completed this year only included one set of data collected in December 2006. To effectively support any conclusions, more data should be analyzed for validation of any conclusions that are drawn.

5 Velocity Ambiguity

5.1 Overview

Velocity Ambiguity is a problem in radar signal processing where received signals from different velocities have a phase shift of greater than 2π . If this were to happen, the phase from the received signal would end up giving a negative velocity, causing anomalies in the data.

When a signal is sent from the radar, it has a specific phase and power. When it encounters an object, a fraction of the power is reflected and the phase is offset by some amount. This phase shift is measured when the signal is returned and from it, we can figure out the velocity the target is moving at from an earlier discussed equation.

The maximum velocity that can be measured by a radar is given by:

$$V_{\max} = \frac{\lambda}{4T}$$

where λ is the wavelength of the transmitted pulse, and T is the pulse repetition period.

Typically, pulsed Doppler radar systems operate at medium to high pulse repetition frequencies (PRFs), which can offset measurements received by the radar. In past years, there have been techniques that have been developed to help correct these ambiguities, such as a clustering algorithm, which will be discussed here.

A popular choice for radar systems has been the Chinese Remainder Theorem. For accurate measurements, this theorem provides accurate results. However, if there is some range error, then the result could have a very large, incorrect value. To help correct this, a clustering algorithm has been researched and implemented. In response to this, a clustering algorithm has been researched and has been shown to perform much better than the Chinese Remainder Theorem.

5.2 Solution Researched

This clustering algorithm takes an array of measurements:

$$V_{ki} = V_i + K V_{ai}; \quad K = \frac{-V_{max}}{V_{ai}}, \dots, \frac{V_{max}}{V_{ai}}$$

where V_{ai} is the Nyquist velocity for a certain PRF, K is a scalar value from the given range, and V_{max} is the maximum magnitude of the target velocity. Once this vector has been created, we order it from smallest to largest and then find the average squared error of the function by:

$$C_R(j) = \frac{1}{m} \sum_{i=j+1}^{i=j+m} \{V_{oi} - \bar{V}\}^2$$

where m is the number of consecutive ordered ranges, V_{oi} is the ordered vector of velocity measurements, and \bar{V} is the median value of the data vector. The minimum value of this resulting vector represents the best grouping of data and by taking the ratio of this to the second lowest value, we can find out the overall probability that its' estimate is correct or not [5]. This algorithm has already been implemented over the summer by Joe Weismann and has been checked over.

How clustering performs given different numbers of PRFs (between 3-6 different, spaced relatively evenly between 1 – 2 kHz) was researched. Comparing 6 PRFs to 3 didn't show too much improvement overall when looking at mean error and standard deviations between multiple realizations. 50 velocities between -45 to 45 m/s 50 times were simulated. Thus, if clustering were to be incorporated into radar systems, a maximum of 3 PRFs should be used over the CRT algorithm, as even with 3 PRFs, it performs much better than the CRT, as seen below.

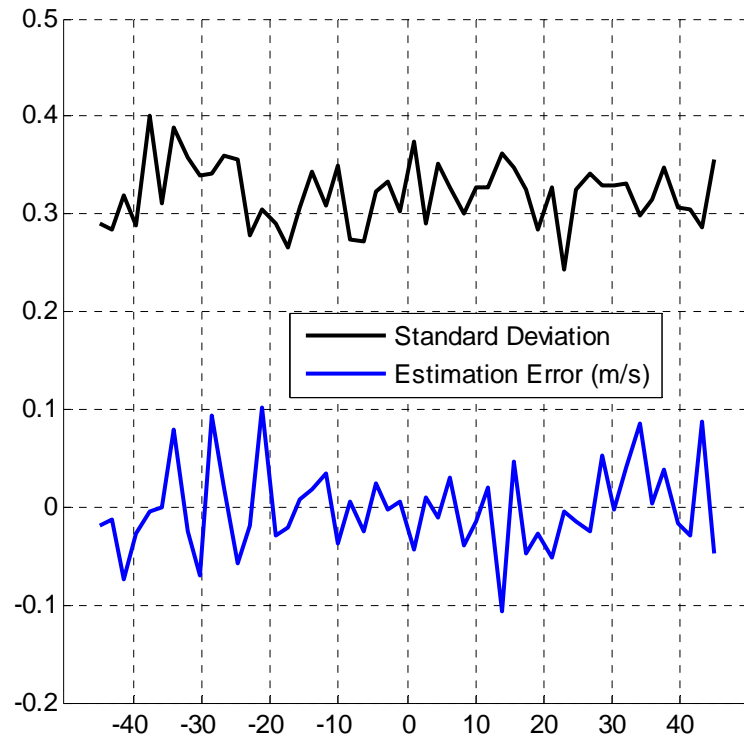


(Figure 23)

The above plot is generated versus the true velocities. The overall error is very, very close to 0. Plotting the estimation error (true velocity – estimated velocity) of the CRT gives a graph in which the clustering algorithm’s performance cannot be seen, from the large error generated by the CRT unfolding technique, as seen in the following graph:

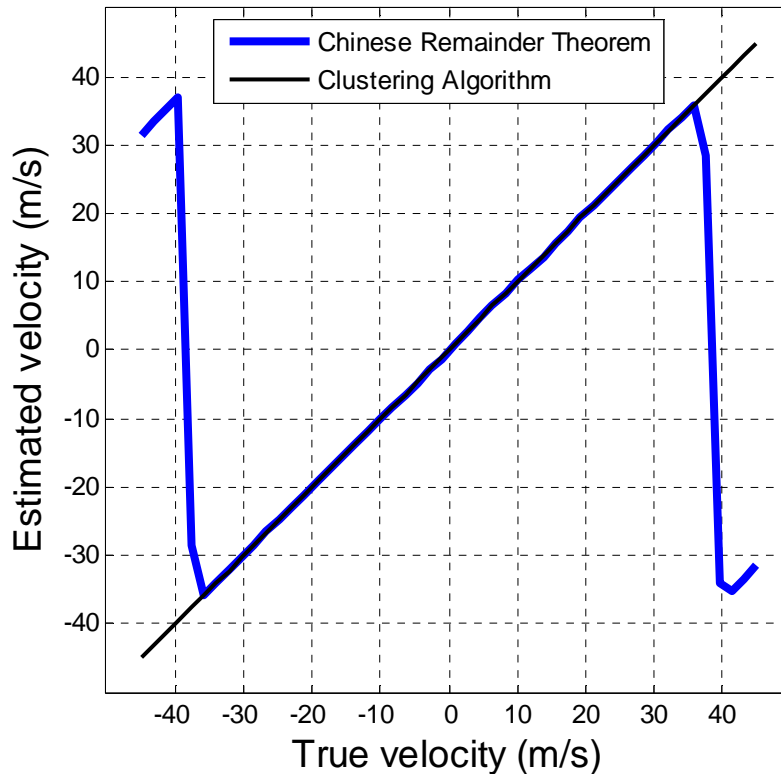


(Figure 24)

The CRT algorithm works fine between -30 to 30 m/s, but then generates very, very large errors beyond those velocities.

Next, it was planned to look at implementing the maximum likelihood technique, which takes an array of data and discriminates between ghost results (ambiguities) and real targets. The results presented in the *Ambiguity Resolution of Multiple Targets Using Pulse-Doppler Waveforms* looked promising, as the calculated probability of successfully resolving up to 4 targets for a medium-PRF waveform was essentially 1. It is also extendable to high PRF applications, with promising success [4].

Going over the algorithm itself, the total likelihood is a function of the probability of detection, the probability of a false alarm, the measurement error characteristics, and the probability of target resolution on a single PRF, which is a function of the target separation from

other targets [6]. This was very difficult to calculate, since some of these factors are unknown, and implementation was difficult – so much so that I was unfortunately unable to implement this algorithm.

What was understood of the maximum likelihood is that the total probability that a radar detection is an actual target, and not a “ghost” target, is given as the probability of obtaining a specified number of false alarms at some velocity, as well as the probability of a false alarm at a given range and the range measurement likelihood for all targets. All of this is performed after clustering the resulting detections into two “groups” as one set of “feasible targets” – super targets, which are composed of more than 3 targets, and another group that consists of 3 measurements, both of which have the smallest possible mean squared error, as per the clustering method.

To calculate the resulting probability, certain aspects need to be known about the radar system, in general. For example, the probability of a false alarm in a given range-Doppler cell and the velocity measurement error variance associated with a given target need to be known. How these are actually calculated or estimated are not mentioned anywhere in the paper – the only comment about these parameters is that in a good pulse-Doppler radar system the probability of false alarms should be small.

Another part of this maximum likelihood method involves calculating various “target combinations” for the given set of feasible targets, i.e. calculating the probability that all detections are false alarms, calculating the probability of one-target combinations, and so forth. For example, for a given two-target combination considerations are made that neither are a “super target,” that only one is a “super target,” or that both are, reordering the targets within these sets while keeping both targets’ mean squared error to a minimum. This process is repeated

for every possible target combination within the set of feasible targets. It's assumed that we are to arbitrarily assign these target combinations in a sort of linear search pattern as we go through the detection set, but no details were given. If this line of thinking is correct, then a programmer would be doing a large number of combination calculations that are very time consuming, as the number of feasible targets is not known until the algorithm is run. Generally, you can set a maximum number of detections that have 3 targets with a minimized squared error, but the set of super targets isn't limited, so depending on your limited set of numbers, the resulting calculations could take a very long time, or a very short time. However, the higher your limit is, the more accurate the algorithm is. The paper chose to use 10 as the maximum size of targets.

5.3 Conclusion

In the end, there were too many unknowns in the probability equation that were glossed over in the research paper, and was unfortunately unable to get the maximum likelihood algorithm running. The clustering portion that was written works fine, however actually calculating the probability is the portion that was unclear. If possible, the maximum likelihood algorithm should be investigated a bit more to find these vague parameters and see if it performs well enough to warrant actual implementation on future hardware updates. Until then, clustering works very well and should definitely be implemented once CHILL or other radars are equipped with the ability to send and receive 3 or more PRFs.

6 Conclusions and Future Work

This year we have barely scratched the surface of the problems that others must face on a daily basis. The problems of clutter, range ambiguity, and velocity ambiguity are not topics that we had learned already in the electrical engineering department but with the help of Professor Chandrasekar, Cuong Nguyen, and Nitin Bharadwaj, we were able to analyze radar data and draw conclusions from this data.

As we have discussed in detail previously, there are different techniques that can be utilized to lower or eliminate the effects of clutter, range ambiguity, and velocity ambiguity. With clutter, FIR and IIR notch filters can be used to eliminate low frequency noise. Also, FFT and GMAP techniques can be used for effective filtering of clutter. Analysis shows that a very effective way of removing ground clutter without worrying about removing wanted signal is the GMAP adaptive filtering. Although not proven to take out all the ground clutter, it is shown that it can be very effective. Research on different data sets can be implemented to exactly see how effective GMAP is with weather targets.

Range ambiguity can be dealt with using phase coding. Although different types of phase coding have been introduced in the past twenty years, today, SZ coding has shown in simulations to be the most effective. Analysis of radar data collected from the CHILL radar in late 2006, showed inconclusive evidence to support the effectiveness of random or SZ phase coding. Two suggestions were made for future continuation of studying range ambiguity: increase the PRF to a frequency which clearly exhibits second trip signals and analyze much more data. Using these two suggestions would likely result in a clearer picture of the efficiency of phase coding.

Finally, velocity ambiguity effects can be lowered using multiple pulse repetition frequencies in conjunction with clustering algorithms and the maximum likelihood estimator. It was impractical to run these methods using real data, as gathering data with more than 2 PRFs is difficult to do, and would require a lot of time to reconfigure the radar to do so. In the end, simulations were run to test the effectiveness overall of clustering and the maximum likelihood, if it could have been coded to work. Due to a lot of ambiguity in the research paper, the maximum likelihood algorithm was unable to be coded and tested, although clustering was analyzed a bit more, and it was concluded that implementation in real radar systems should be done, if the potential to gather more than 2 PRFs exists.

Over the course of the past school year, we were able to first learn the basic problems involved in processing data obtained from radars (clutter, range ambiguity, velocity ambiguity) and then learned about methods to minimize these issues. These problems will always exist when processing radar data, but with more research and data analysis, it will be possible to significantly reduce their negative effects.

7 REFERENCES

- [1] Siggia, A.D and Passarelli, Jr. R. E. *Gaussian model adaptive processing (GMAP) for improved ground clutter cancellation and moment calculation: ERAD*, 2004
- [2] Skolnik, Merrill I. Introduction to Radar Systems. 2nd ed. New York: McGraw-Hill, 1980.
- [3] Sachindananda, M., Zrnic, D., “Systematic Phase Codes for Resolving Range Overlaid Signals in a Doppler Weather Radar,” *Journal of Atmospheric and Oceanic Technology*, vol. 16, issue 10, pp. 1351-1363, October 1999.
- [4] Trunk, Gerard; Kim, Moon, “Ambiguity Resolution of Multiple Targets Using Pulse-Doppler Radar” *.IEEE Transactions on Aerospace and Electronic Systems*, vol. 30, no. 4, pp. 1130-1137, October 1994.
- [5] Trunk, G.; Brockett, S. “Range and Velocity Ambiguity Resolution”. *IEEE*, 1993.
- [6] Weissman, Jonathan. “Velocity Ambiguity Mitigation with Staggered PRF”.

8 BIBLIOGRAPHY

Gubner, John A. Probability and Random Processes for Electrical and Computer Engineers.

Cambridge: Cambridge UP, 2006.

Hanselman, Duane. The Student Edition of MATLAB. 5th ed. Upper Saddle River, NJ: Prentice

Hall, 1997.

Ingle, Vinay K., and John G. Proakis. Digital Signal Processing Using MATLAB. Pacific Grove,

CA: Brooks/Cole Company, 2000.

Oppenheim, Alan V., Ronald W. Schafer, and John R. Buck. Discrete-Time Signal Processing.

2nd ed. New York: Pearson Prentice Hall, 1999.

Peebles, Peyton Z., and Bruce Littlefield. Radar Principles. New York: John Wiley & Sons,

1998.

Rinehart, Ronald E. Radar for Meteorologists. 2nd ed. Fargo: Knight Printing, 1991.

Siggia, A.D and Passarelli, Jr. R. E. *Gaussian model adaptive processing (GMAP) for improved ground clutter cancellation and moment calculation*: ERAD, 2004

A1 Relevant Matlab codes

File: bimodal.m

```
% This file creates radar clutter for a given signal that is similar
% to example.m.
% This file calls the simSIG.m file that was provided to us

clc
clear all
close all

%*****
% Input parameters for S-band radar data
f0=3e9;           % Radar frequency in Hz ( X-band ~10 GHz,
                  S-band ~3 GHz)
c=3e8;           % Velocity of light m/s
lambda=c/f0;    % Wavelength in m
prt=1e-3;
prf=1/prt;

fmax=1/(2*prt); % Nyquits freq.
va=lambda/(4*prt); % Unambiguity radial velocity
rmax=c*prt/2;   % Unambiguity range

m=64;           % Sample size
pn=15;         % Noise power (in dB)
SNR=20;        % Signal to noise ratio (in dB)
p=pn+SNR;      % Signal power (in dB)
v=5;          % Signal velocity (in m/s)
w=4;          % Signal spectrum width (in m/s)

% Dual-polarization parameters
rhoco_P=0.99;  % Co-polar correlation coefficient of
                signal
phidp_P=-50;  % Differential propagation phase in deg
zdr_P=2;      % ZDR for precipitation in dB

win_flag=1;    % Set window effect for simulation program
                (1: apply window effect on the data; 0:
                no)
noise_flag=1;  % Indicate wheather noise is included in
                simulated data or not (1: yes; 0: no)

warning off;
format short;

%*****
% Generate data
% h_ts: time series for H polarization signal
% v_ts: time series for V polarization signal
[h_ts,v_ts]=simSIG(f0,prt,m,p,pn,v,w,zdr_P,phidp_P,rhoco_P,noise_flag,win_flg);
```

```

pn=15;
SNR=40;
p=pn+SNR;
v=0;
w=.1;
[h_clut,v_clut]=simSIG(f0,prt,m,p,pn,v,w,zdr_P,phidp_P,rhoco_P,noise_flag,win
_flag);

h_temp=convn(h_ts,h_clut,'same');
v_temp=convn(v_ts,v_clut,'same');

%*****
% Plot PSD of the signal (Hamming Window)

[Phh,faxis] = periodogram(h_ts,hamming(m),m,fmax);
vaxis=fliplr(linspace(-va+2*va/m,va,m));

Phh=fftshift(Phh);

% Signal with Clutter
[ph_temp,fax_temp]=periodogram(h_temp,hamming(m),m,fmax);
vax_temp=fliplr(linspace(-va+2*va/m,va,m));

ph_temp=fftshift(ph_temp);

figure
subplot(2,2,1), plot(vaxis,dbs(Phh),'r-',vax_temp,dbs(ph_temp))
legend('Red line: Without Clutter','Blue line: With Clutter');
grid on;
xlabel('Velocity (ms^{-1})')
ylabel('Power (dB)')
title('Hamming window')

%*****
% Plot PSD of the signal (Blackman window)

[Phh,faxis] = periodogram(h_ts,blackman(m),m,fmax);
vaxis=fliplr(linspace(-va+2*va/m,va,m));

Phh=fftshift(Phh);

% Signal with Clutter
[ph_temp,fax_temp]=periodogram(h_temp,blackman(m),m,fmax);
vax_temp=fliplr(linspace(-va+2*va/m,va,m));

ph_temp=fftshift(ph_temp);

subplot(2,2,2), plot(vaxis,dbs(Phh),'r-',vax_temp,dbs(ph_temp),'b-')
legend('Red line: Without Clutter','Blue line: With Clutter');
grid on;
xlabel('Velocity (ms^{-1})')
ylabel('Power (dB)')
title('Blackman Window')

%*****
% Plot PSD of the signal (Rectangular Window)

```

```

[Phh,faxis] = periodogram(h_ts,rectwin(m),m,fmax);
vaxis=fliplr(linspace(-va+2*va/m,va,m));

Phh=fftshift(Phh);

% Signal with Clutter
[ph_temp,fax_temp]=periodogram(h_temp,rectwin(m),m,fmax);
vax_temp=fliplr(linspace(-va+2*va/m,va,m));

ph_temp=fftshift(ph_temp);

subplot(2,2,3), plot(vaxis,dbs(Phh),'r-',vax_temp,dbs(ph_temp))
legend('Red line: Without Clutter','Blue line: With Clutter');
grid on;
xlabel('Velocity (ms^{-1})')
ylabel('Power (dB)')
title('Rectangular Window')

```

File: spectrumage.m

```
% DESCRIPTION: creates time series data with length m; calculate and plot the
mean power and mean velocity, as well as the variations of both; uses the
simSIG.m file provided to us for signal generation
% INPUT: power of noise; SNR; velocity; spectrum width.

%*****
% Input parameters for S-band radar data
f0=3e9;           % Radar frequency in Hz ( X-band ~10 GHz, S-band
~3 GHz)
c=3e8;           % Velocity of light m/s
lambda=c/f0;     % Wavelength in m
prt=1e-3;
prf=1/prt;

fmax=1/(2*prt);  % Nyquist freq.
va=lambda/(4*prt); % Unambiguity radial velocity
rmax=c*prt/2;    % Unambiguity range

m=64;            % Sample size
pn=15;           % Noise power (in dB)
SNR=20;          % Signal to noise ratio (in dB)
p=pn+SNR;        % Signal power (in dB)
v=5;             % Signal velocity (in m/s)
w=4;             % Signal spectrum width (in m/s)

% Dual-polarization parameters
rhoco_P=0.99;    % Co-polar correlation coefficient of signal
phidp_P=-50;     % Differential propagation phase in deg
zdr_P=2;         % ZDR for precipitation in dB

win_flag=1;      % Set window effect for simulation program (1:
apply window effect on the data; 0: no)
noise_flag=1;    % Indicate wheather noise is included in
simulated data or not (1: yes; 0: no)

warning off;
format short;

%*****
% Generate data in a two-dimensional array, h_signal(row,column)
% h_ts: time series for H polarization signal
% v_ts: time series for V polarization signal
% Also calculate Mean Power, Mean Velocity
% psd_ts: Mean Power
% vel_ts: Mean Velocity

temp=1;
n_samp=16:16:256; % Sets our X Axis in # of samples
psd_ts=zeros([1,5]);
vel_ts=zeros([1,5]);
std_p=zeros([1,5]);
psd_temp=zeros([25,5]);
vel_temp=zeros([25,5]);
std_p=zeros([1,5]);
```

```

std_v=zeros([1,5]);

for i=16:16:256;
    for j=1:25

[h_ts,v_ts]=simSIG(f0,prt,i,p,pn,v,w,zdr_P,phidp_P,rhoco_P,noise_flag,win_fla
g);
        [h_temp,h_lag]=xcorr(h_ts,1);
        psd_temp(j,temp)=h_temp(2)/i;
        vel_temp(j,temp)=phase(h_temp(3));
    end
    temp=temp+1;
end
vel_temp=abs(vel_temp * lambda/(4*pi*prt));
psd_ts=mean(dbs(psd_temp));
vel_ts=mean(vel_temp);
std_p=std(dbs(psd_temp));
std_v=std(vel_temp);

%*****
% Plots
%

figure
plot(n_samp,psd_ts,'o-');
grid on;
xlabel('Number of Samples');
ylabel('Mean Power (dB)');

figure
plot(n_samp,vel_ts,'o-');
grid on;
xlabel('Number of Samples');
ylabel('Mean Velocity');

figure
plot(n_samp,std_p,'o-');
grid on;
ylabel('std(P)');
xlabel('Number of Samples');

figure
plot(n_samp,std_v,'o-');
grid on;
xlabel('Number of Samples');
ylabel('std(Velocity)');

```

A2 Additional Considerations

The project was split into three subprojects with Joe Hoatam studying clutter suppression, Aaron Nielsen studying range ambiguity, and Josh Merritt studying velocity ambiguity mitigations. Additional guidance on these specific topics was provided by Cuong Nguyen, and Nitin Bharadwaj.

Though project cost might be an important consideration in other projects, our project was focused around researching improvements to the software analyzing the radar data. No project costs were involved in this research. Future costs involved in this project would only involve software updates.

This project was geared towards weather radar data signal processing, thus the target audience is quite limited. Some of the methods mentioned earlier could be extended to other radar uses such as military projects.

A3 Acknowledgements

This semester we have worked with several students and faculty members that have been extremely helpful in our studies. Our overall guidance for this project was from Dr. Chandrasekar. Two graduate students, Cuong Nguyen, and Nitin Bharadwaj, were responsible for our week to week progress and critique of our weekly presentations. Members of CHILL such as Jim George and Pat Kennedy were helpful in giving us CHILL on-site technical information. Finally, Olivera Notaros provided overall direction. These people have all been very beneficial in our project this semester.